


# Abatement of Aerosols by Ionic Wind Extracted From Dielectric Barrier Discharge Plasma

Tehreem Arshad<sup>1</sup>, Muhammad Shahid Rafique<sup>1</sup>, Shazia Bashir<sup>2</sup>, Asma Hayat<sup>2</sup>, Muhammad Ghulam Murtaza<sup>1</sup>, Abdul Muneeb<sup>1</sup>, Imran Shahadat<sup>1</sup> and Nabiha Nayab<sup>1</sup>

<sup>1</sup>Department of Physics, University of Engineering and Technology, Lahore, Pakistan.

<sup>2</sup>Department of CASP, Government College University Lahore, Pakistan.

Environmental Health Insights  
Volume 18: 1–12  
© The Author(s) 2024  
Article reuse guidelines:  
sagepub.com/journals-permissions  
DOI: 10.1177/11786302241262879



**ABSTRACT:** Lahore (Pakistan), being an industrial city, has high emission of aerosols that affects and contaminates the air quality. Therefore, the abatement/inactivation of aerosols is necessary to restrict their infectious activities. In this project, ionic wind isolated from dielectric barrier discharge plasma (DBD plasma) has been utilized to abate the aerosols trapped in the Surgical Mask and KN95 Respirator. To infer the chemical and elemental detection of ambient aerosols, FTIR and LIBS have been employed. "From the results, it is noteworthy that abatement/removal of aerosols has been successfully carried out by the ionic wind irradiation and highlights the potential of DBD plasma technology in removing the aerosols pollution."

**KEYWORDS:** Dielectric barrier discharge plasma (DBD-plasma), ionic wind, aerosols, particulate chemical composition, FTIR, LIBS

**RECEIVED:** March 6, 2024. **ACCEPTED:** May 30, 2024.

**TYPE:** Environmental Health Education: New Trends, Innovative Approaches and Challenges - Original Research

**FUNDING:** The author(s) received no financial support for the research, authorship, and/or publication of this article.

**DECLARATION OF CONFLICTING INTERESTS:** The author(s) declared no potential conflicts of interest with respect to the research, authorship, and/or publication of this article.

**CORRESPONDING AUTHOR:** Tehreem Arshad, Department of Physics, University of Engineering and Technology, Lahore 54890, Pakistan. Email: tehreemmarshad44@gmail.com

## Introduction

The presence of atmospheric aerosols (solid and/or liquid particulates in a gas) has a variety of consequences on human health,<sup>1</sup> climate, and visibility.<sup>2</sup> Several studies have found a link between particulate matter inhalation and negative health effects, the importance of which is mostly determined by chemical composition, particle size, and exposure period. Furthermore, long-term exposure to a polluted environment has been associated with an increased risk of cardiovascular disease and death. Because they influence cloud formation and the global radiative balance, atmospheric aerosols significantly impact climate.<sup>3</sup>

Aerosols pollute our environment disapprovingly—the increased concentration of aerosols in the air quality demands a productive technique to control pollution measures. This project aims to abate/break the chemical structure of aerosols for inactivation purposes. Therefore, the DBD techniques are considered innovative techniques that have the tremendous potential to inactivate/eliminate aerosols. The DBD technologies offer outstanding practical applications for aerosols disinfection as air purifiers and can be used in hospitals, industries, and factories where the risks of aerosols emissions are dominant.

Atmospheric aerosols are made up of a complex mix of components with different ranges in size,<sup>4</sup> emission sources, physical properties, and chemical compositions.<sup>5</sup> Several studies have shown that atmospheric aerosols are enriched with nitrate, ammonium, sulfates,<sup>6,7</sup> organic elements, heavy metals, sea salt, and black carbon.<sup>8</sup> These particulates also consist in the form of compounds such as alkenes, methyl, carboxylic

acids, aldehydes, carbohydrates, lactones, ketones, esters, ammonium sulfate as well as ammonium nitrates.<sup>9–12</sup>

Particulate Matter (PM) and Primary Biological Aerosol (PBA) are the subsets of atmospheric aerosols.<sup>5</sup> PM is a major determinant of indoor air quality and is defined as the sum of all solid and liquid particles suspended in the air.<sup>13</sup> The elements that participate in the composition of PM include Copper (Cu), Aluminum (Al), Chromium (Cr), Zinc (Zn), Cadmium (Cd), Lead (Pb), Mercury (Hg), etc.<sup>14</sup> Since the industrial revolution, a significant rise in air pollution has been observed on local, regional, and global levels. Heavy concentrations of gaseous contaminants including ozone and nitrogen oxides are lethal to people's health<sup>4</sup> because they cause respiratory, allergic, and cardiovascular diseases.

PBA has been described as a major problem that poses a threat to the environment and international health standards. Toxic elements, such as volatile organic compounds (VOCs), heavy metals, and harmful gases, can be found in bioaerosols.<sup>15</sup> The main elemental composition includes Sodium (Na), Calcium (Ca), Iron (Fe), Phosphorous (P), and Potassium (K), etc.<sup>14,16</sup> Aerosols consist of different types of biological aerosols, volatile organic compounds (VOCs), and inorganic matters.

To reduce the exposure of airborne aerosolized microorganisms, different types of masks have been used as Personal Protective Equipment (PPE).<sup>17,18</sup> It is recommendable to use face masks during the Severe Acute Respiratory Syndrome Coronavirus pandemic,<sup>19</sup> for protection from infectious diseases caused by aerosols and pathogenic particles. The use of masks has been acting as the first-line



defense against aerosolized pathogens. Masks or any type of filters (Quartz filters, HEPA, ULPA) is useful to filtrate the airborne particulates<sup>10,20,21</sup> but they do not inactivate the aerosols.<sup>22</sup>

Many techniques have also been utilized to inert the activities of aerosolized particulates such as ozone-water (OW) spray,<sup>23</sup> ultraviolet germicidal irradiation (UVGI),<sup>24</sup> photocatalytic oxidation,<sup>25</sup> and Plasma methods (arc plasma, DBD plasma).<sup>15,22,26</sup> Plasma methods have a great potential to abate and/or remove the aerosols (VOCs, PBA). Xiao et al<sup>27</sup> investigated the abatement of VOCs by non-thermal plasma. Gao et al<sup>28</sup> used the atmospheric pressure plasmas for effective abatement of PBA. Li et al<sup>29</sup> summarizes the various applications of DBD non-thermal plasma on the abatement of VOCs. Timmermann et al,<sup>30</sup> checked the combined effect of DBD with the ionic wind for indoor air purification. Prehn et al<sup>22</sup> also investigated the plasma treatment and ionic wind effect for inactivation of bacteria for air purification. Ionic wind extracted from the DBD reactor is one of the effective methods to abate and/or inactivate the aerosols. For this purpose, a system was devised that uses non-thermal DBD plasma combined with ionic wind to overcome the drawbacks of filter technology.<sup>31</sup>

## Experimental Setup

The aim of this project is to abate/remove the ambient aerosols by ionic wind extracted from DBD plasma. In order to collect the aerosols from the ambient environment, surgical mask (Waterlink Pakistan (Pvt) Ltd. Pakistan) and KN95 respirator (H3 Traders, Pakistan) have been used as filter. These samples have been chosen due to the difference in their materials, fiber diameter, and the filtration capacity of the medium to trap the ambient aerosols.<sup>32</sup>

### Experimentation

The pristine masks were placed at 70 m above the ground level for 20 days during January 2022. The reason for choosing the winter season is that there is abundance of fog and smog which we believe are the major sources of aerosols. The weather conditions during January 2022 in Lahore, Pakistan were; temperature  $\sim 10^{\circ}\text{C}$  to  $15^{\circ}\text{C}$ , pressure 1016 to 1020 mbar, humidity 60% to 80%, and visibility 3 to 5 km.

Figure 1 shows the micrographs of (a) pristine of surgical mask, (b) air-exposed surgical mask, (c) pristine of KN95 respirator, (d) air-exposed KN95 respirator. It is clear from the figure that the aerosols have been trapped in both the filters (b and d). For the abatement of collected aerosols with ionic wind, a DBD plasma setup has been designed and fabricated. Air-exposed samples were then irradiated with the ionic wind produced by the DBD plasma reactor.

A schematic configuration, real time image, and circuit diagram of the DBD setup is presented in Figure 2. The DBD reactor comprises of 2 electrodes made of

copper ( $180\text{ mm} \times 70\text{ mm} \times 5\text{ mm}$ ), a dielectric (ceramic;  $180\text{ mm} \times 70\text{ mm} \times 2\text{ mm}$ ) placed between 2 electrodes, and a high-voltage AC power supply (homemade, 30 kV, 50 Hz). An AC input of 12 and 20 kV is applied to upper electrode, which is perforated. The perforation is done because ions from plasma will be made to pass through this electrode. The separation between the 2 electrodes is 2 mm. An electric field is established in the discharge gap that equals or exceeds the breakdown strength of the ambient air. Plasma is formed in the form of micro-discharge filaments that carries temperature  $\sim 39.045\text{ eV}$ , density  $3.87 \times 10^{20}\text{ m}^{-3}$ , and frequency  $8.77 \times 10^{11}\text{ Hz}$  evaluated by using Langmuir Probe. Plasma includes excited species, collection of molecules, EM radiations, free radicals, ions, and electrons. To extract the ions from the plasma, another electrode was used as an extraction electrode (copper;  $180\text{ mm} \times 70\text{ mm} \times 5\text{ mm}$ ) placed above the perforated electrode at a distance of 20 mm. In order to extract the ions, the third electrode was negatively biased ( $-15\text{ kV}$ ) DC.

The purpose of the extraction of ions (named as ionic wind) from the plasma was to irradiate these ions on the air-exposed surgical mask and KN95 respirator. Furthermore, the impact of irradiation of ionic wind on the abatement of aerosols trapped in the filters (Figure 1b and d) has been explored. The reason to choose the ionic wind rather than the plasma itself to treat the pollutants is to avoid the ozone as the DBD plasma produces more ozone concentration.<sup>30,33</sup> Whereas ions while traveling toward the extraction electrode, interact with the air molecules and produce many active substances, such as oxidizing species  $OH$ ,  $O$ ,  $NO^{-2}$ ,  $NO^{-3}$ ,  $NO^{\bullet}$ ,  $O_3$ ,  $HO^{\bullet}$ ,  $O_2^{-}$ , etc. These species are considered the sources to abate the aerosols.

### Confirmation of ionic wind

In order to confirm the formation of ionic wind, a CR-39 track detectors were placed at the extraction electrode. Plasma was formed and ions were made to fall on the CR-39. After the exposure, CR-39 was etched in NaOH solution (6.25 N, 8 hours,  $70^{\circ}\text{C}$ ) and cleaned by sonication method. The formation of the tracks was observed by optical microscope. Figure 3 is the micrographs of CR-39 confirming the development of ion tracks, which evidences of the ionic wind.

### Ionic wind irradiation on air-exposed surgical mask and KN95 respirator

Furthermore, air-exposed samples (surgical mask & KN95 respirator) were placed at the extraction electrode and irradiated with the ionic wind. The choice for isolating ions from the plasma channel is because of the large mass of the ions. They transfer the momentum to the pollutants that rupture their

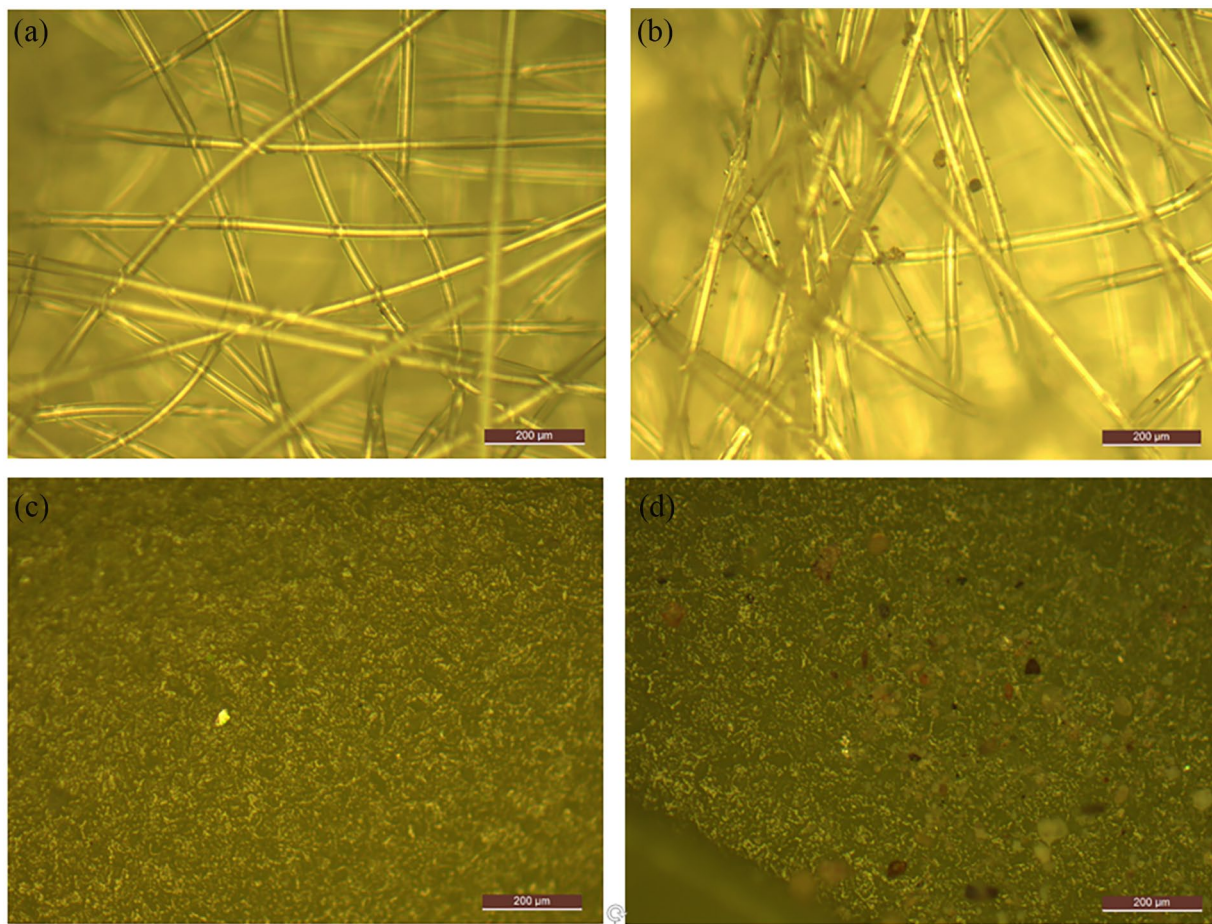


**Figure 1.** Optical micrographs: (a) pristine surgical mask, (b) air-exposed surgical mask, (c) pristine KN95 respirator, and (d) air-exposed KN95 respirator.

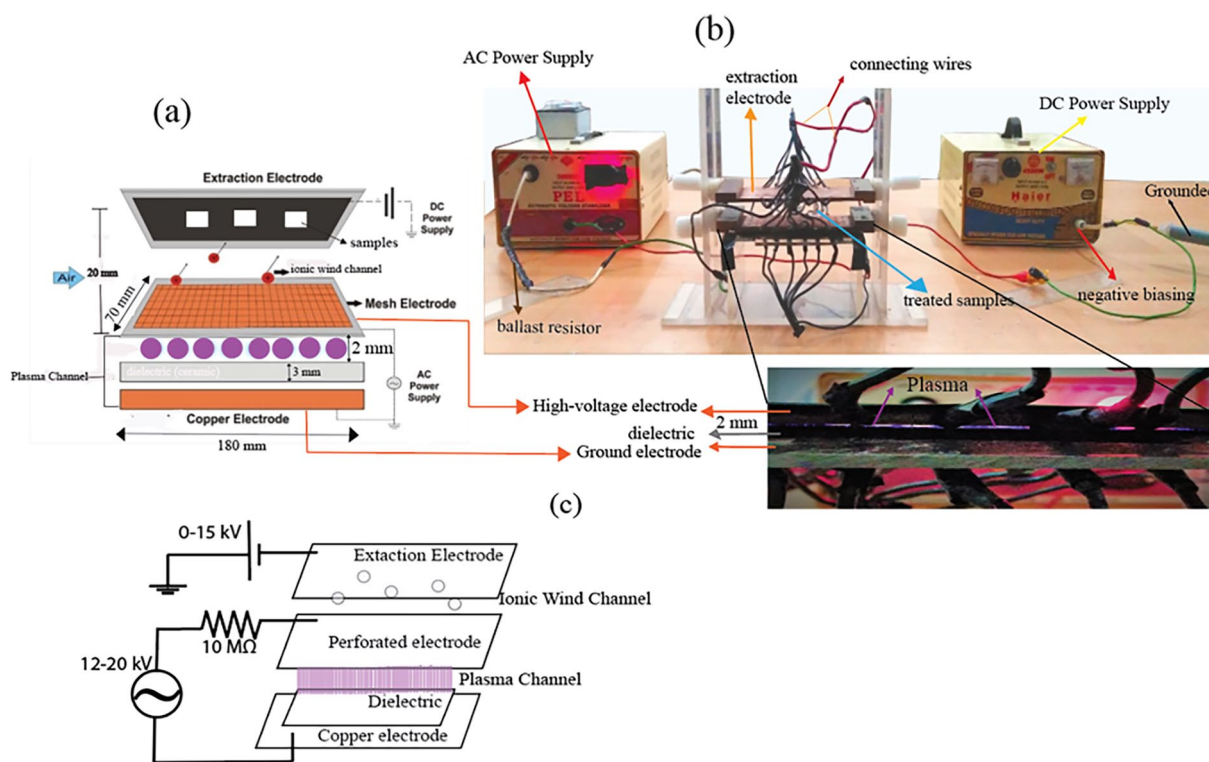


**Figure 2.** (a) Schematic representation, (b) real-time image, and (c) circuit diagram of dielectric barrier discharge plasma combined with ionic wind extraction electrode.

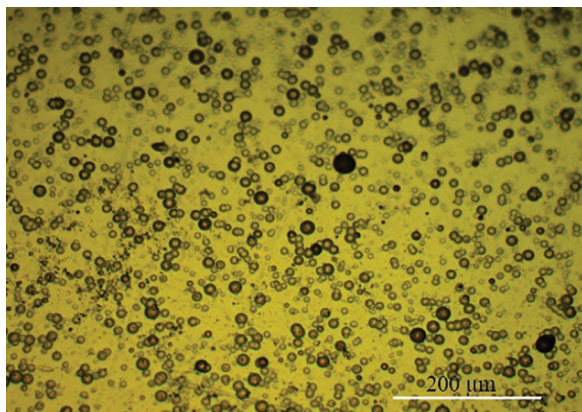


**Figure 3.** Optical micrograph of CR-39 showing the pattern of ionic wind.

chemical composition. Moreover, ions interact with the air molecules and produce many active substances, such as oxidizing species and free radicals, etc. These species are also considered the sources to abate/remove the chemical structure of aerosols. The experiment was carried out at 12 and 20 kV of AC voltage for a fixed irradiation period of 20 minutes. Herein, the main objective was to investigate the effects of the input voltage on the abatement of aerosols by the ionic wind.

## Result and Discussion

To abate the trapped aerosolized particles, the surgical masks and KN95 respirator have been bombarded with the ionic wind emitted from the DBD plasma reactor. Some mechanisms for the abatement of aerosols by low-temperature and non-equilibrium plasma have been explained and discussed. Physical processes in the discharge stream caused by ionic wind play an important role in abatement/inactivation purposes. On the other hand, low-energy ions generate the free radicals, excited atomic and molecular species that start up the chemical reactions, which in turn, deactivate the targeted air pollutants by decomposing their chemical structure. The pristine, air-exposed, and ionic wind irradiated samples have been analyzed by FTIR and LIBS techniques.

### FTIR analyses

Fourier transform infrared spectroscopy (FTIR) has been employed to identify the organic and inorganic functional groups of ambient aerosols. The spectrum of a chemical substance obtained from the IR spectroscopy, is like a photograph of a molecule. It is an easy approach to extract the structural information of aerosols and the chemical changes, which is occurred due to different ionic wind treatments. FTIR spectra of the aerosols composition of untreated and ionic wind treated were recorded. Spectra of the samples were obtained over wavenumber between 4000 and 650  $\text{cm}^{-1}$  with 4  $\text{cm}^{-1}$  resolution by averaging 96 scans.

**Surgical masks.** Figure 4 exhibits the IR spectra obtained for pristine (a), air-exposed (b), ionic wind irradiated surgical mask

at 12 kV (c), and ionic wind irradiated surgical mask at 20 kV (d). The pristine spectrum (4a) shows a broad band at the wavenumbers from 3000 to 2800  $\text{cm}^{-1}$ , identified as a C-H (alkanes) group. Another peak is dominated at the wavenumber of 1500 to 1350  $\text{cm}^{-1}$  and is recognized as C-H (alkanes) group. The presence of C-H group is due the polypropylene, which is the constituent material of the surgical mask. A bunch of peaks observed at 1200 to 700  $\text{cm}^{-1}$  belongs to C-O and C=C (alkenes) group. The presence of C-O might be due to the oxidation.<sup>34</sup>

FTIR spectrum for the air-exposed sample in Figure 4b exhibits the characteristic peaks associated with alkanes, fluoro compounds, amines, ethers, sulfonates/sulfates, alkenes, and halocompounds. Four spectral ranges have been recognized in the air-exposed sample at 3000 to 2800, 1500 to 1300, 1300 to 1000, and 1000 to 700  $\text{cm}^{-1}$ . The increase in the intensity of absorbing bands within 3000 to 2800  $\text{cm}^{-1}$  peaking at approximately 2952, 2914, 2870, and 2840  $\text{cm}^{-1}$  corresponds to the C-H (alkanes) group in the spectrum for the air-exposed sample. An additional weak peak appears at 2700  $\text{cm}^{-1}$  is assigned as C-H group.

At 1500 to 1300  $\text{cm}^{-1}$ , there exists 2 strong peaks. Several plausible assignments are possible between the narrow region at 1470 to 1350  $\text{cm}^{-1}$  comprising C-H (alkanes), C-F (fluoro compounds), and S=O (sulfonates/sulfates) groups. At 1453  $\text{cm}^{-1}$ , methylene groups ( $\text{CH}_2$ ) have a particular bending absorption. In addition, at 1375  $\text{cm}^{-1}$ , methyl groups ( $\text{CH}_3$ ) contain a characteristic bending absorption. A strong peak of asymmetric stretching of sulfonyl chlorides also occurs at 1375  $\text{cm}^{-1}$ . At the region from 1400 to 1300  $\text{cm}^{-1}$ , functional groups of sulfonate, sulfones, sulfonamides, and sulfate are also expected.<sup>35</sup> These identified groups are the main ingredients that participate in the formation of photochemical smog.<sup>9</sup>

Some others peaks belonging to C-O and C-N groups have also been observed in the region of 1300 to 1000  $\text{cm}^{-1}$ . There is one peak of C-O group that is associated to the ethers. Esters and alcohols give an absorbing peak in this region too. However, this possibility is eliminated by observing the absence of the O-H band.<sup>35</sup> Another functional group C-N is expected in this region. The C-N group also occurs in the range between 1350 and 1000  $\text{cm}^{-1}$ . Therefore, the functional group at 1162  $\text{cm}^{-1}$  is assigned to C-N (amines) and/or C-O (ethers).

Two peaks are also observed in the region between 1000 and 700  $\text{cm}^{-1}$ . The C=C vibrations at this region appear as a weak absorbing band. Bending absorption of C=C (alkenes) group is observed at 998 and 991  $\text{cm}^{-1}$ . At 850 to 700  $\text{cm}^{-1}$ , there may exist some halocompounds such as C-Cl, C-Br, and/or C-I bands. Two peaks at 842 and 805  $\text{cm}^{-1}$  have been observed and assigned to C-Cl (halocompounds).<sup>9,10,36</sup>

The contribution of alkanes, sulfonates, sulfones, sulfonamides, ethers, fluoro compounds, amines, alkenes and halocompounds confirms that the mask has trapped the aerosolized particles.<sup>6,8,12</sup> The presence of hydrocarbons (CH group), oxides of sulfur and nitrogen particulates, and

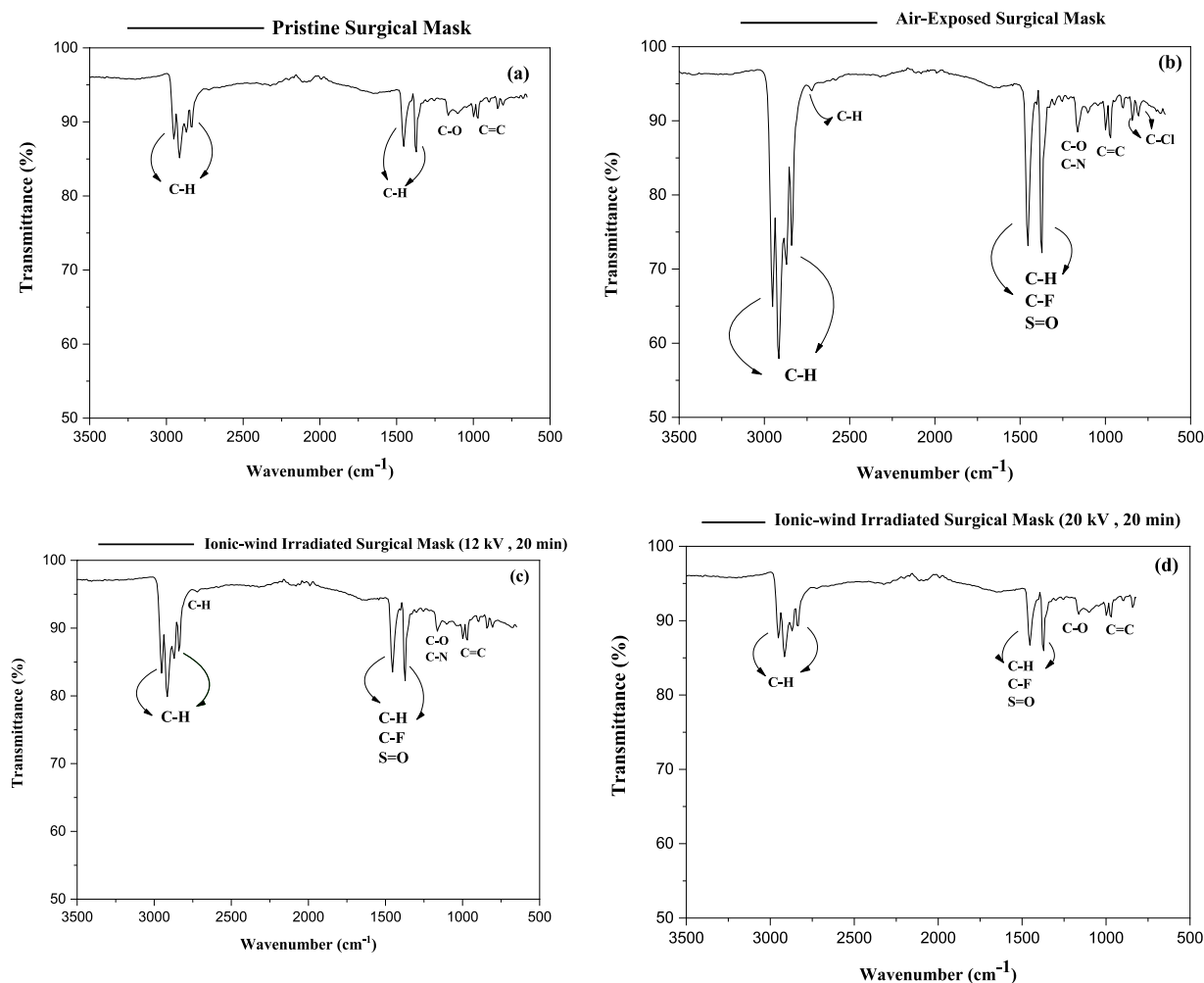


**Figure 4.** IR spectra of surgical mask: (a) pristine, (b) air-exposed, (c) air-exposed surgical mask irradiated with the ionic wind at 12 kV, and (d) air-exposed surgical mask irradiated with the ionic wind at 20 kV.

chlorofluorocarbons, makes the air toxic. Identified compounds also participate in the formation of VOCs (Toluene, Acetone, Benzene, Xylene, diethylether, aliphatic hydrocarbon, chlorinated compounds such as P-chlorophenol, P-cumene, aldehydes such as formaldehyde and acetaldehyde, and Dichloromethane, etc.),<sup>9,37-39</sup> and biological aerosols' development.<sup>40,41</sup>

South Asia is highly prone to the harmful impacts of increasing aerosols amount due to population growth, fast urbanization, increase in motorized traffic, and expanding industrialization both inside and outside of metropolitan areas. Both anthropogenic and natural sources are responsible for producing aerosols. Natural aerosols like sea salt and dust mainly arise from the southern dry regions as well as the nearby ocean while anthropogenic aerosols mostly originate from industrial and vehicular emissions.

Pakistan, located in the northwestern part of South Asia, is also influenced by the growing aerosols concentration. Nevertheless, only a few investigations have been performed on long-term aerosols patterns in Pakistan, so far. Lahore, a highly populated city of Pakistan, is an industrial city, including small and medium industries. Sources of aerosols are the emission of

VOCs from industry, soil or dust particulates, emissions from vehicles and from the burning of crop residues in the nearby areas.<sup>42</sup> Many researchers have investigative studies on the aerosols data over Lahore.<sup>43-46</sup>

Ambient aerosols act as the seed for the formation of clouds and fog. Nevertheless, excess concentration results in negative effects on natural phenomena. Photochemical smog, air contamination, and several impacts on the microphysics of clouds, nitrogen, global carbon, and sulfur are caused due to the presence of aerosols.<sup>46</sup> Many different compounds are included in VOCs such as benzene, acetone, chlorinated hydrocarbons, monocyclic aromatic hydrocarbons (MAHs)<sup>37</sup> and toluene, xylene, and ethylbenzene,<sup>47</sup> etc., some of which may have negative short- and long-term health impacts.

Ionic wind approaches are receiving increasing attention as a means of degrading different kinds of gaseous contaminants. The abatement of aerosols was carried out by ionic wind emitted from a planer DBD plasma. Samples were treated at 12 and 20 kV of AC voltage applied across the electrodes for a fixed time duration of 20 minutes while the DC voltage at 15 kV was kept constant. Spectra of the air-exposed surgical masks irradiated with ionic wind exhibit a significant reduction in peak

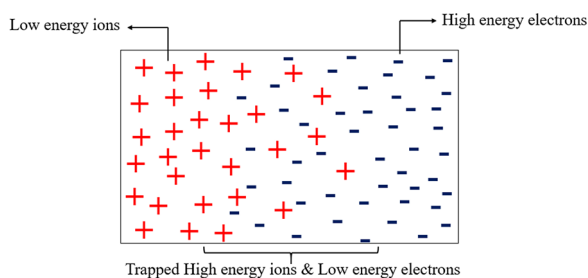


**Figure 5.** Schematic representation of self-generated electric field and trapped electrons and ions in plasma.

intensities of all the functional groups as compared to the air exposed samples (Figure 4c and d).

In Figure 4c, the ionic wind irradiated sample at an applied voltage of 12 kV and discharge current (~3 to 4 mA) depicts the reduction in the intensity of characteristic peaks corresponding to alkanes, fluoro compounds, sulfonates/sulfates, amines, and halocompounds as compared to air-exposed sample. A decrease in the intensity at the 4 spectral ranges 3000 to 2800, 1500 to 1300, 1300 to 1000, and 1000 to 700  $\text{cm}^{-1}$  points out that ionic wind damages the aerosols molecular chemistry. Ions extracted from DBD plasma interact with many organic and inorganic elements of aerosols through oxidation<sup>48</sup> and by other chemical and physical mechanisms.<sup>30</sup> The principles behind the abatement of aerosols with ionic wind induced from non-thermal plasma like DBDs may be explained by the fact that the low energy ions (50–200 eV in our case) activate surrounding ambient gas molecules. Different collision processes subsequently start many reactions generating free radicals such as O,  $\text{NO}_2^-$ ,  $\text{NO}_3^-$ ,  $\text{NO}\cdot$ ,  $\text{O}_3$ , etc., for decomposing pollutants/aerosols.<sup>49,50</sup> Oxidation is the primary method for decreasing exhausts including the dilute concentration of contaminants (NO, VOC) in the mixture of  $\text{N}_2$  and  $\text{O}_2$ . The observed decrease in the absorption peaks is due to the change in structure by ionic wind-induced chemical reactions.<sup>29,39,48</sup>

Figure 4d illustrates the spectrum for an ionic-wind irradiated sample operated at 20 kV and discharge current (3–4 mA). In this case, the peaks observed at the same wavenumber as those for 12 kV appear to have much less intensity. The kinetic energy of the electrons increases with higher voltage and more energy is transferred from the electron to the neutral atom because of collisions. The self-generated electric field is formed because of the collection of localized low energy ions and localized high energy electrons separately. Due to this electric field, high energy ions and low energy electrons are trapped, resulting in the increased collection of ions and electrons. The increase in collision between ions and electrons gives rise to the plasma temperature. Figure 5 shows the schematic representation of self-generated electric field in plasma. Furthermore, in order to extract ions from plasma, while traveling from plasma to extraction electrode, electrons collide with the other species, which will give rise to the temperature too. Plasma's temperature rises due to a strong self-generated electric field and thus ejecting more ions. The ions effectively

dissociate the molecules for abatement purposes. The structure of exposed aerosols is quickly damaged by the ionic wind bombardment at higher (as compared to at 12 kV) ion fluxes.

In conclusion, ionic wind treatment at an applied voltage of 20 kV demonstrated encouraging results for the decomposition of many aerosols constituents. Energetic ions produced by the DBD channel react with the air molecules in the pathways. On collisions, free radicals and more ions are generated and interact with the captured aerosols. It is simple to understand that a higher applied voltage causes higher ionic current pulses. It happens because of a higher field being attained and more powerful partial discharges being triggered which leads to the abatement of aerosols.

*KN95 respirator.* Figure 6 presents the IR spectra of pristine (a), air-exposed (b), and ionic wind irradiated at 20 kV (c) obtained for the KN95 respirator. FTIR spectrum for the pristine filter in Figure 6a indicates the absorption band at 3000 to 2800  $\text{cm}^{-1}$  peaking at 2966  $\text{cm}^{-1}$  belonging to the C-H group. In the range of 1500 to 650  $\text{cm}^{-1}$ , there are some prominent and intense peaks, showing an absorption at 1408  $\text{cm}^{-1}$  assigned to C-H, at 1260 and 1050  $\text{cm}^{-1}$  related to C-O group, and C=C at 780  $\text{cm}^{-1}$ . These absorption bands relate to polypropylene, a polymer that is used in surgical mask.<sup>34</sup>

Figure 6b presents the IR spectrum of air-exposed filter/KN95 respirator. At 3200  $\text{cm}^{-1}$ , a low intensity shoulder appears that corresponds to the N-H band. A complete identification of compound classes has been performed by analyzing the 4 characteristics regions with large absorbance peaks at 3000 to 2800, 1800 to 1400, 1300 to 1000, and 1050 to 650  $\text{cm}^{-1}$ . At 3000 to 2800  $\text{cm}^{-1}$ , strong absorbing band of C-H (alkane) group has been found peaking at 2959, 2922, and 2870  $\text{cm}^{-1}$ . This shows that the molecular structure of trapped particles contains the large concentration of hydrocarbon such as methylene group/methane group. At 1800 to 650  $\text{cm}^{-1}$ , there exists a wide region having sharp and medium peaks representing different functional groups. A strong absorption peak appears at 1722  $\text{cm}^{-1}$  that corresponds to the C=O (carbonyl) group. C=C has a weak absorption at approximately 1595, 1550, 1453, and 954  $\text{cm}^{-1}$ . Nitro groups show 2 bands in the IR spectrum, which appears at 1513  $\text{cm}^{-1}$  and the other peak at 1356  $\text{cm}^{-1}$ . Several compound classes such as S=O (sulfates/sulfones), C-O (ethers), C-N (amines), and C-F (halocompounds) are in the range 1350 to 1200  $\text{cm}^{-1}$ .<sup>7–9</sup> In addition, a medium absorbing band appears in the spectrum at 1125 and 1066  $\text{cm}^{-1}$  that can be associated to C-N and C-F groups. The bands observed at 745 and 696  $\text{cm}^{-1}$  are related to the C-Cl vibrations.<sup>10,51,52</sup>

The intensity of the peaks that were existing in the pristine sample has been increased in the case of air-exposed sample. Furthermore, the additional peaks have been observed in the air-exposed sample that shows the more vibrations of functional groups due to the captured aerosols.

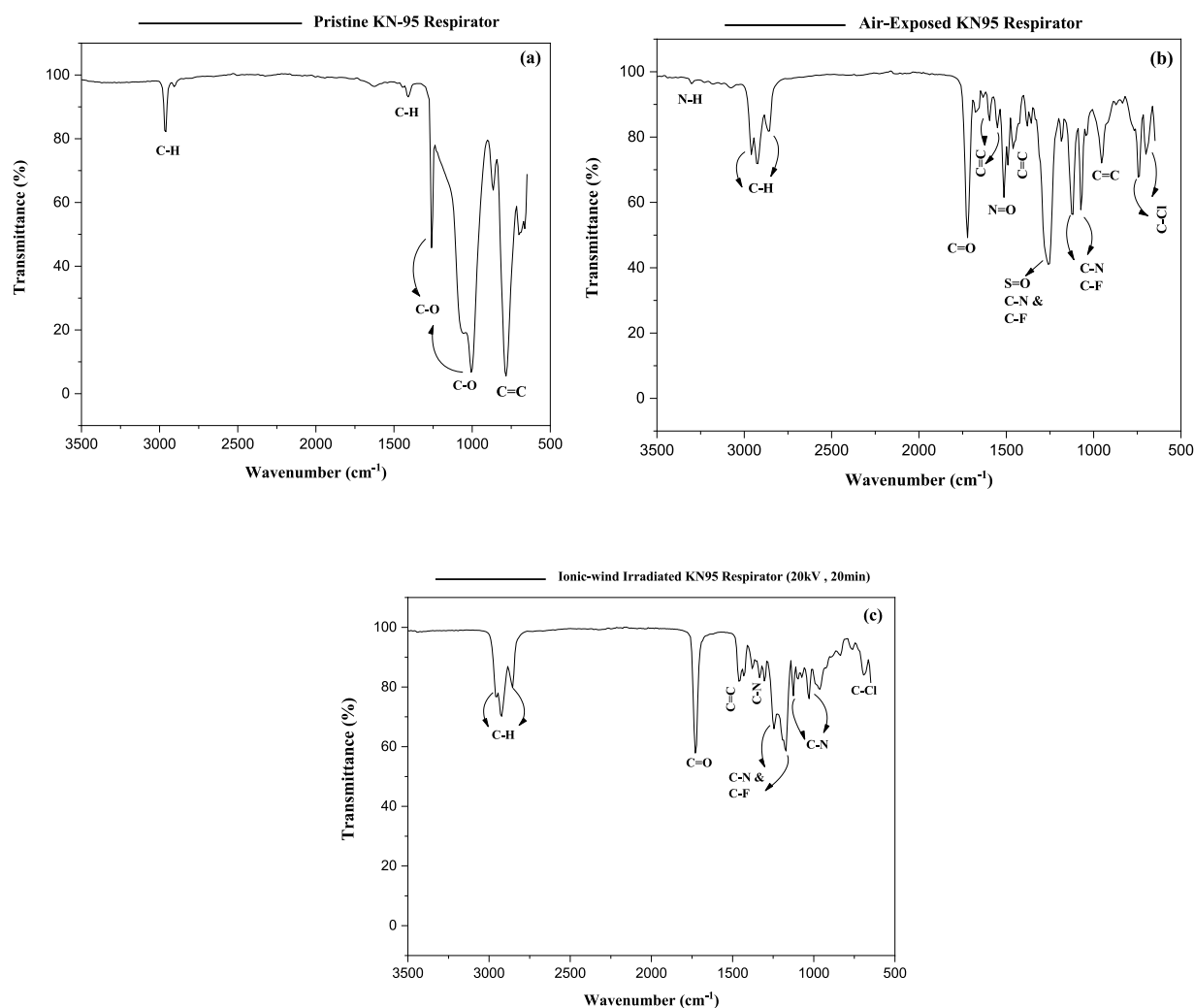


**Figure 6.** IR spectra of KN95 respirator: (a) pristine, (b) air-exposed, and (c) air-exposed KN95 respirator irradiated with the ionic wind at 20 kV.

Keeping in view the results obtained in the case of surgical mask, the air-exposed KN95 respirator was irradiated only by the ionic wind produced at 20 kV, since 20 kV was favorable to abate the chemical composition of aerosols effectively. As compared to the ambient sample, the spectrum of the ion irradiated KN95 respirator revealed a reduction in the aforementioned peaks (Figure 6c). Absorbance band peaking at 1722 and 1453  $\text{cm}^{-1}$ , which was nominated as C=O and C=C respectively, shows a reduction in intensity. A medium absorbing intensity of C-N and C-F appears at 1244 and 1177  $\text{cm}^{-1}$ . A slight shift in the position at 1125 and 1036  $\text{cm}^{-1}$  of absorbing peaks and reduction in intensity has been observed that indicates the presence of C-N group. Less vibrations of functional groups and reduction in the intensity of chemical bonds as compared to the ambient samples suggests that the ionic wind has successfully abated the molecular chemistry of aerosols. Because of strong electric fields, generation of ions as well as the collisional processes between ionic wind and surrounding air molecules generate free radicals, which are responsible to destabilize and decompose the aerosols due to their high reactivity.<sup>27</sup>

Many classes of oxygen, hydrogen, carbon and nitrogen-containing compounds have been detected in almost all the air-exposed spectra for both the cases surgical mask and KN95 respirator. These classes include the organic compounds such as alkanes, carboxylic acid, amines, esters, nitrocompounds, ethers, halocompounds, and alkenes. In addition to organic compounds, there were some inorganic compounds like sulfates, nitrates, and sulfuric acids present, as suggested by spectrum information. The purpose of this project was to abate these toxic compounds by irradiation of ions extracted from the DBD plasma. Most of the organic and inorganic compounds has been eradicated/removed after ionic wind irradiation.

Moreover, to cross-check the reduction in aerosols against the ion-flux, Laser induced breakdown spectroscopy has also been employed.

#### *Laser induced breakdown spectroscopy (LIBS) analyses*

In order to further explore the elemental detection of aerosols deposited on filters and their abatement after the ionic wind

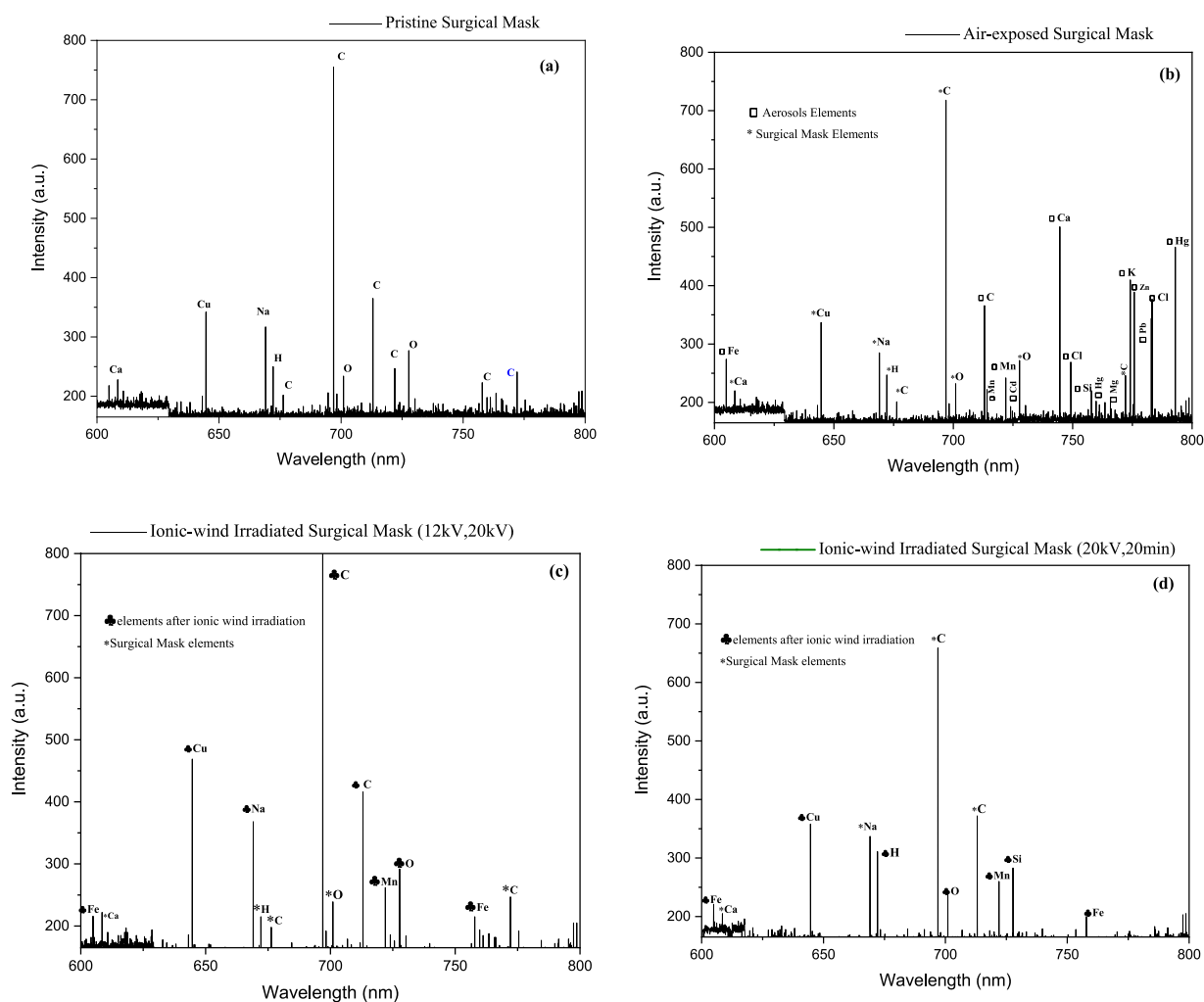


**Figure 7.** LIBS spectra of surgical mask: (a) pristine, (b) air-exposed, (c) air-exposed surgical mask irradiated with the ionic wind at 12kV, and (d) air-exposed surgical mask irradiated with the ionic wind at 20kV.

irradiation, LIBS technique has been employed. Detection of metals and metalloids in volatile organic compounds (VOCs) or primary biological aerosols (PBA) that comes from anthropogenic sources and through vehicles emission easily figure out by LIBS technique.<sup>53</sup>

**Surgical mask.** Figure 7 represents the LIBS single-shot spectra of the surgical mask. Figure 7a illustrates the LIBS spectrum of pristine surgical mask, presents the several emission lines between 600 and 800nm. Emission lines of elements such as of Cu appears at 644.6 nm, Na at 668.90 nm, and C at 696.94 and 713.1 nm have more intense peaks as compared to Ca at 608.667 nm, H at 672.13 nm, and O at 701.60, 727.74 nm. The surgical masks are made from the synthetic material, polypropylene ( $C_3H_6$ )<sub>n</sub>. Therefore, presence of C and H elements represents the constituent of the filter material.<sup>54</sup> Elements such as Cu, Ca, Na have also been observed in the pristine spectrum, which shows antibacterial and antiviral properties to polypropylene.<sup>55,56</sup>

Identification of C, H, and O has also been observed in the FTIR pristine spectrum of surgical mask. By employing the

LIBS technique, additional elements have been detected that participate in the manufacturing process of surgical masks.

Figure 7b displays a spectrum of air-exposed surgical mask. This spectrum shows the high concentration of metallic/semi metallic components like Fe, C, Mn, Cd, Ca, Cl, Si, Mg, S, Pb, Hg, and K in addition to the elements that were present in the pristine surgical mask. Because masks are made of polypropylene, therefore C, H, and O signals is distributed in the entire samples (pristine, air-exposed, ionic wind irradiation). The emission lines were found to be the most intense related to Fe (604.94 nm), C (713.06 nm), Ca (744.63 nm), K (774.10 nm), Zn (775.79 nm), Cl (783.25 nm), S (792.97 nm), and Hg (792.97 nm), identified by National Institute of Standards and Technology (NIST) atomic spectra database lines data. Identification of metallic components in large proportion suggests the deposition of aerosols over the surgical mask/filter which are main constituents of the ambient aerosols.<sup>57</sup>

Aerosols cause air pollution, smog, and different effects on the cloud's microphysics, sulfur, nitrogen, and global carbon in both direct and indirect ways. Large concentration of heavy metals in ambient air coming from industrialized and highly



urbanized areas participate in the formation of  $PM_{2.5}$ . Elements such as Pb, Cl, and Ca suggest the impact of traffic emissions, incinerator emissions, and fossil fuel combustion. The presence of Pb is also associated to the industrial processes/man-made activities such as non-ferrous metal industries. S appears in the air samples is attributed due to the photochemical smog as well as combustion of diesel and fuel oil. Identified elements such as C, Mn, Cl, Fe, Ca, and K is also related to the biological aerosols.<sup>58-60</sup> The presence of elements like O, S, C, Zn, Pb, and Fe are found as constituents of photochemical smog.<sup>61-63</sup> Furthermore, elements such as Ca, Mg, Fe, Mn, Si, and K presents the elemental trace of biological aerosols, and metallic elements like Cd, Ca, Cr, Pb, Si, K, Fe, Zn, and Hg are considered the trace of  $PM$ .<sup>41</sup>

FTIR results also confirms the detected elements such as C, H, S, O, Cl but by employing LIBS technique, additional information regarding elemental detection can be determined.

The detected elements in aerosols including all heavy metals are considered harmful. Chronic exposure to such air-toxics has many negative health effects, as they buildup in the body tissues. Long-term contact with salts or oxides can result in acute or long-term poisonings, tumors, disorders of the cardiovascular, and nervous systems as well as some elements weaken human immunity.<sup>64</sup> Atmospheric aerosols significantly influence the climate and atmospheric chemistry. Aerosols have an impact on the planet's radiation balance, which has effects on the climate.  $PM$  directly scatter or absorb the sunlight, or indirectly by contributing atomic nuclei to the formation of cloud droplets and ice particles, which alters the reflectivity and lifespan of the cloud.<sup>65</sup> Therefore, it is necessary to break/abate their molecular structure for inactivation purposes. The air-exposed masks were then irradiated with the ionic wind extracted from the DBD plasma. As, it is observed in the FTIR results, applied voltages of AC at 12 and 20 kV showed the significant impact on the abatement of aerosols. Ions and radical groups attack the nitrogen and oxygen molecules directly in the air. It destroy  $N_2$  and  $O_2$  to form oxidizing agents and nitrogenous by-products, which effectively abate the molecular structure of aerosols.

Figure 7c illustrates a spectrum of the ionic wind irradiated sample at 12 kV of AC. The spectrum shows a significant reduction in the atomic emission lines as compared to air-exposed samples. Emission lines from Pb, Cd, Ca, Cl, Si, K, Zn, and Mg have been vanished, as they were present in the air-exposed sample. Since, the C (696.93 nm) signal is a constituent of the surgical mask and its signal appears in all of the cases. However, it is more intense in the ionic wind irradiated sample at 12 kV. Emission line of C is quite intense rather to the other detected elements, suggests that the captured aerosols have enriched with the organic content. Increase in the intensity levels of Cu (644.66 nm), Na (669.078 nm), Mn (721.99 nm), O (727.75 nm), and Si (757.84 nm) have been observed due to the abated molecular structure of aerosols by

ionic wind irradiation. As it is discussed above in the results of FTIR spectroscopy that ions generated at the higher voltages creates more oxidizing agents and nitrogen oxides. These active species interact with the targeted sample and damage their molecular structure. To further lessen the elements, air-exposed samples were exposed once again with ionic wind at 20 kV of AC.

Figure 7d displays a spectrum for the ionic wind irradiated sample at 20 kV, which shows the further reduction in the intensity of elements such as Cu (644.80 nm), Na (668.9 nm), C (699.94 nm, 713.11 nm), O (727.74 nm), and Si (757.84 nm), which appeared in the spectrum of ionic-wind irradiated at 12 kV. The reason behind the less atomic emission is that at the higher voltages such as 20 kV, generates more oxidizing agents, nitrogenous by-products and chemical reactions, which effectively abate the molecular composition of aerosols. In addition, the intensity and number of current pluses increases at higher voltages that easily remove the aerosols. The chemical bonds of aerosols' molecules are easily destroyed due to the strong electric field and many active species. This means that aerosols are more fully decomposed.

Although, some of the toxic elements in aerosols are found by FTIR analysis. However, LIBS is a more powerful technique for analyzing the elemental detection. Additional elements such as Zn, Pb, K, Cd, Cl, Cu, Na (constituent of aerosolized particles) have been observed in the LIBS spectra. Thus, ionic wind extracted from DBD Plasma deactivation kinetics has reduced the original concentration of aerosols, as predicted by the less emission lines/elemental detection by employing LIBS techniques.

*KN95 respirator.* Figure 8 shows the LIBS spectra obtained in the different cases for KN95 respirator. Figure 8a illustrates the elemental peaks obtained for pristine KN95 respirator/filter. Emission lines from Na at 604.80 nm, Cu at 644.66 nm, O at 701.00 nm, and 727.75 nm, H at 672.13 nm, and C at 696.94, 713.1, and 772.12 nm, shows the elemental constituent of the respirator.<sup>54-56</sup> Figure 8b shows the LIBS spectrum of the air-exposed KN95 respirator. According to the graph, new additional atomic emission lines of N, Fe, Si, C, Ti, S, and Pb are present in rather high content. Additionally, this spectrum shows that Na, Cu, C, H and O emission lines, which are present in all of the spectra. These elements are the constituents of KN95 respirator/filter. Emission line at 618.67 nm relates to N, 638.67 and 760.07 nm belong to Fe, at 666.756 to Si, at 732.12 nm to Ti, at 744.63 to S, and at 782.90 nm relates to Pb, according to National Institute of Standards and Technology (NIST) atomic spectra database lines data. Detection of new elements in the air-exposed sample suggests that they are arises from the captured aerosols. Elemental detection shows that the aerosols are composed of these heavy metals. The release of such air toxics have negative effects on human respiratory system<sup>41</sup> as well as contaminate the air quality.<sup>66</sup> In order to abate

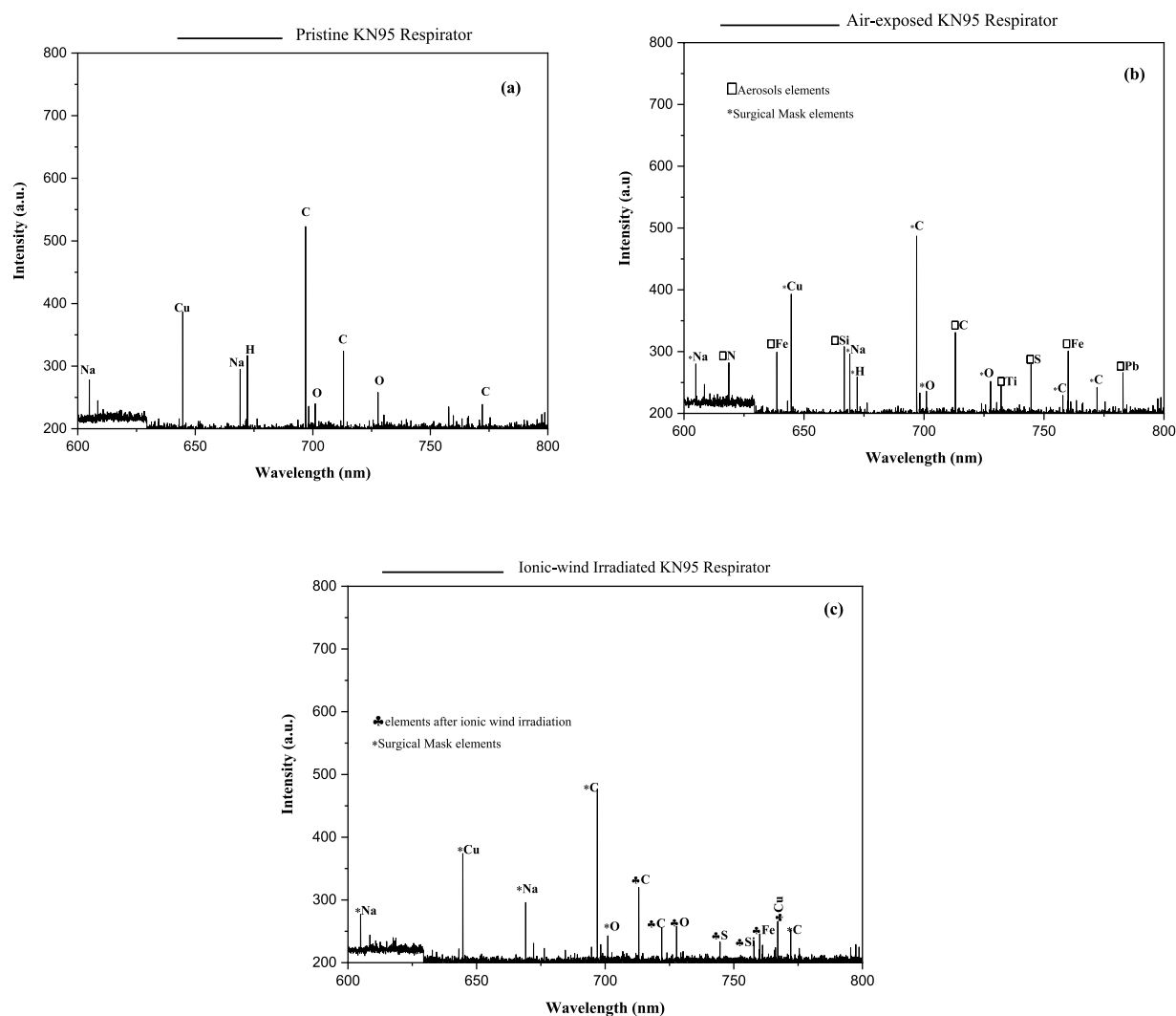


**Figure 8.** LIBS spectra of KN95 respirator: (a) pristine, (b) air-exposed, and (c) air-exposed KN95 respirator irradiated with the ionic wind at 20kV.

the molecular structure, ionic wind has been applied to the aerosols captured by the filter (KN95 respirator). Irradiation exposure at 20kV for 20 minutes has been provided as it is found (in the case of surgical mask) that the higher voltage is significant for the abatement of aerosols. Figure 8c shows the LIBS spectrum of ionic-wind irradiated at 20kV. Emission lines corresponds to the elements such as N, Fe, Ti, Si, and Pb have been eliminated after the ions bombardment. A large number of active species is generated through the plasma-activated ions, which break the chemical bonds as well as decompose the molecular structure of aerosols.

The adaptable method of Laser Induced Breakdown Spectroscopy (LIBS) allows for quick multi-elemental detection analyses. The identification of the chemical composition by LIBS is because each element has its unique spectral emission signals, measured in LIBS range (600–800 nm). The composition of ambient aerosols and its abated elemental detection has been observed by quantifying the major elements in filter samples through the laser induced breakdown spectroscopy.<sup>57,67</sup> Elements such as C, O, and H that forms

the organic matter and/or water, were identified. The investigation demonstrated that S, Ca, Hg, Cl, Ti, Fe, Mg, K, Si, Pb, Cd, and Na were the main metallic/semimetallic components in aerosols along with H and C associated with organic matter, inorganic salts, elemental carbon and/or water. Ionic wind methods of DBD plasma is a suitable candidate that eliminate/abate the chemical structure of aerosols. High-voltage electrical discharges directly generate many active groups that destabilizes the molecular structure of aerosols. The ozone and nitrogenous byproducts produced from the ionic wind, break the molecular chemistry of aerosols very easily. It is observed in all cases that the LIBS pattern of the samples after the treatment have less atomic emission than those of samples before treatment.

On the behalf of the results from FTIR and LIBS, mostly organic content was found in the ambient filter and a very few amount of inorganic matter. After the ionic wind treatment, less concentration of metallic and/or metalloids elements have been found, which suggests the successful results of the ionic wind on the abatement of ambient aerosols.

## Conclusion

In conclusion, an efficient method to abate/remove/eradicate the ambient aerosols has been explored. Ionic wind extracted from the DBD plasma was used to abate the molecular composition of aerosols. For this purpose, aerosols were trapped from the ambient environment using the medical mask (surgical and KN95). Air-exposed samples have been irradiated with ionic wind at 12 and 20kV of AC voltage by keeping the constant exposure period of 20 minutes. There is a notable reduction in the strength of functional groups in the ions-irradiated sample as compared to air-exposed regardless of the operating potential. However, the reduction is more prominent in the case of ions irradiated at 20kV of applied voltage. Moreover, the intensity of atomic emission lines of aerosols decreased when samples were exposed to the ionic wind. This investigation has shown the optimal condition for lowering the majority of chemical components at 20kV for a fixed time of 20 minutes. DBD plasma-activated ionic wind is an efficient way for the remediation/abatement/eradication of aerosols/contaminated air. It can be installed in the industries and factories where the chances of emission of aerosols are higher.

## Author Contributions

It is mentioned that all authors contributed their infrastructure and services to the completion of this project's work, including the experimental setup, design, material preparation, experimentation, and analysis. TA (corresponding author) has participated in this project in all respects. MS (Research Supervisor) has guided me logically in all respects and has significant contributions to this project. TA, MS, IS, MG, and Abdul Muneeb have participated in experimental setup designing and fabrication. TA and NN have contributed to the preparation of samples. TA, MS, SB, and AH have helped in performing the LIBS experiment and analyses.

## ORCID iD

Tehreem Arshad  <https://orcid.org/0000-0002-2946-4138>

## REFERENCES

- Shiraiwa M, Ueda K, Pozzer A, et al. Aerosol health effects from molecular to global scales. *Environ Sci Technol.* 2017;51:13545-13567.
- Xiong J, Zhao T, Bai Y, et al. Climate characteristics of dust aerosol and its transport in major global dust source regions. *J Atmos Sol Phys.* 2020; 209:105415-105426.
- Kumar P, Pratap V, Kumar A, et al. Assessment of atmospheric aerosols over Varanasi: physical, optical and chemical properties and meteorological implications. *J Atmos Sol Phys.* 2020;209:105424-105437.
- Lowther SD, Deng W, Fang Z, et al. How efficiently can HEPA purifiers remove priority fine and ultrafine particles from indoor air? *Environ Int.* 2020;144:106001-106010.
- Su H, Cheng Y, Pöschl U. New multiphase chemical processes influencing atmospheric aerosols, air quality, and climate in the anthropocene. *Acc Chem Res.* 2020;53:2034-2043.
- Weakley AT, Takahama S, Dillner AM. Ambient aerosol composition by infrared spectroscopy and partial least-squares in the chemical speciation network: organic carbon with functional group identification. *Aerosol Sci Technol.* 2016;50:1096-1114.
- Varrica D, Tamburo E, Vultaggio M, Di Carlo I. ATR-FTIR spectral analysis and soluble components of PM(10) and PM(2.5) particulate matter over the urban area of Palermo (Italy) during normal days and Saharan events. *Int J Environ Res Public Health.* 2019;16:2507-2521. doi:10.3390/ijerph16142507
- Takahama S, Johnson A, Russell LM, Takahama S, Johnson A. Quantification of carboxylic and carbonyl functional groups in organic aerosol infrared absorbance spectra. *Aerosol Sci Technol.* 2013;47:310-325.
- Cao G, Yan Y, Zou X, Zhu R, Ouyang F. Applications of infrared spectroscopy in analysis of organic aerosols. *Spectral Anal Rev.* 2018;06:12-32.
- Popovicheva O, Ivanov A, Vojtisek M. Functional factors of biomass burning contribution to spring aerosol composition in a megacity: combined FTIR-PCA analyses. *Atmosphere.* 2020;11:319.
- Claffin MS, Liu J, Russell LM, Ziemann PJ. Comparison of methods of functional group analysis using results from laboratory and field aerosol measurements. *Aerosol Sci Technol.* 2021;55:1042-1058.
- Jiang H, Jang M. Dynamic oxidative potential of atmospheric organic aerosol under ambient sunlight. *Environ Sci Technol.* 2018;52:7496-7504.
- Colbeck I, Lazaridis M. Aerosols and environmental pollution. *Naturwissenschaften.* 2010;97:117-131.
- Cerro JC, Cerdà V, Querol X, et al. Variability of air pollutants, and PM composition and sources at a regional background site in the Balearic Islands: review of western Mediterranean phenomenology from a 3-year study. *Sci Total Environ.* 2020;717:137177-137195.
- Bisag A, Isabelli P, Laurita R, et al. Cold atmospheric plasma inactivation of aerosolized microdroplets containing bacteria and purified SARS - CoV - 2 RNA to contrast airborne indoor transmission. *Plasma Process Polym.* 2020; 17(10):2000154-2000162. doi: 10.1002/ppap.202000154
- Hybl JD, Lithgow GA, Buckley SG. Laser-induced breakdown spectroscopy detection and classification of biological aerosols. *Appl Spectrosc.* 2003;57: 1207-1215.
- Forouzandeh P, O'Dowd K, Pillai SC. Face masks and respirators in the fight against the COVID-19 pandemic: an overview of the standards and testing methods. *Saf Sci.* 2021;133:104995-105006.
- Yim W, Cheng D, Patel SH, et al. KN95 and N95 respirators retain filtration efficiency despite a loss of dipole charge during decontamination. *ACS Appl Mater Interfaces.* 2020;12:54473-54480.
- Tang S, Mao Y, Jones RM, et al. Aerosol transmission of sars-cov-2? Evidence, prevention and control. *Environ Int.* 2020;144:106039-106049.
- Lange R, Dall'Osto M, Skov H, et al. Characterization of distinct Arctic aerosol accumulation modes and their sources. *Atmos Environ.* 2018;183:1-10.
- Zhou SS, Lukula S, Chiosso C, et al. Assessment of a respiratory face mask for capturing air pollutants and pathogens including human influenza and rhinoviruses. *J Thorac Dis.* 2018;10:2059-2069.
- Prehn F, Timmermann E, Kettlitz M, et al. Inactivation of airborne bacteria by plasma treatment and ionic wind for indoor air cleaning. *Plasma Process Polym.* 2020;17:1-12.
- Huang HC, Huang HL, Hsu YF, Yang S. Applying the ozone water spraying for inactivating E. Coli bioaerosols. *IOP Conf Ser Earth Sci.* 2019;310:052027-052032. doi:10.1088/1755-1315/310/5/052027
- Wang C, Lu S, Zhang Z. Inactivation of airborne bacteria using different UV sources: performance modeling, energy utilization, and endotoxin degradation. *Sci Total Environ.* 2019;655:787-795.
- Patil SB, Basavarajappa PS, Ganganagappa N, et al. Recent advances in non-metals-doped TiO2 nanostructured photocatalysts for visible-light driven hydrogen production, CO2 reduction and air purification. *Int J Hydrogen Energy.* 2019;44:13022-13039.
- Lai ACK, Cheung ACT, Wong MML, Li WS. Evaluation of cold plasma inactivation efficacy against different airborne bacteria in ventilation duct flow. *Build Environ.* 2016;98:39-46.
- Xiao G, Xu W, Wu R, et al. Non-thermal plasmas for VOCs abatement. *Plasma Chem Plasma Process.* 2014;34:1033-1065.
- Gao H, Wang G, Chen B, et al. Atmospheric-pressure non-equilibrium plasmas for effective abatement of pathogenic biological aerosols. *Plasma Sources Sci Technol.* 2021;30:053001.
- Li S, Dang X, Yu X, et al. The application of dielectric barrier discharge non-thermal plasma in VOCs abatement: a review. *Chem Eng J.* 2020;388:124275-124299.
- Timmermann E, Prehn F, Schmidt M, et al. Indoor air purification by dielectric barrier discharge combined with ionic wind: Physical and microbiological investigations. *J Phys D Appl Phys.* 2018;51:164003.
- Portugal S, Roy S, Lin J. Functional relationship between material property, applied frequency and ozone generation for surface dielectric barrier discharges in atmospheric air. *Sci Rep.* 2017;7:6388-6411.
- Hill WC, Hull MS, MacCusprie RI. Testing of commercial masks and respirators and cotton mask insert materials using SARS-CoV-2 virion-sized particulates: comparison of ideal aerosol filtration efficiency versus fitted filtration efficiency. *Nano Lett.* 2020;20:7642-7647.

33. Qasim M, Rafique MS, Naz R. Water purification by ozone generator employing non-thermal plasma. *Mater Chem Phys*. 2022;291:126442-126456.
34. Ardila-Suárez C, Pablo Villegas J, Lins de Barros Neto E, Ghislain T, Lavoie JM. Waste surgical masks to fuels via thermochemical co-processing with waste motor oil and biomass. *Bioresour Technol*. 2022;348:126798-126805.
35. Lewis W. Ultraviolet spectroscopy. *Paint Test Man*. 2009;545-545-2.
36. Boris AJ, Takahama S, Weakley AT, et al. Quantifying organic matter and functional groups in particulate matter filter samples from the southeastern United States – part 2: spatiotemporal trends. *Atmos Meas Tech*. 2021;14:4355-4374.
37. Matsumoto K, Matsumoto K, Mizuno R, Igawa M. Volatile organic compounds in ambient aerosols. *Atmos Res*. 2010;97:124-128.
38. Ondarts M, Hajji W, Outin J, Bejat T, Gonze E. Non-thermal plasma for indoor air treatment: toluene degradation in a corona discharge at ppbv levels. *Chem Eng Res Des*. 2017;118:194-205.
39. Chang T, Wang Y, Wang Y, et al. A critical review on plasma-catalytic removal of VOCs: catalyst development, process parameters and synergetic reaction mechanism. *Sci Total Environ*. 2022;828:154290-154317.
40. Zafar N, Shamaila S, Nazir J, et al. Antibacterial action of chemically synthesized and laser generated silver nanoparticles against human pathogenic bacteria. *J Mater Sci Technol*. 2016;32:721-728.
41. Ramli NA, Md Yusof NFF, Shith S, Suroto A. Chemical and biological compositions associated with ambient respirable particulate matter: a review. *Water Air Soil Pollut*. 2020;231:044905-044919. doi:10.1007/s11270-020-04490-5
42. Ali G, Bao Y, Ullah W, et al. Spatiotemporal trends of aerosols over urban regions in Pakistan and their possible links to meteorological parameters. *Atmos*. 2020;11:306.
43. Gupta P, Khan MN, da Silva A, Patadia F. Modis aerosol optical depth observations over urban areas in Pakistan: quantity and quality of the data for air quality monitoring. *Atmos Pollut Res*. 2013;4:43-52.
44. Ali M, Tariq S, Mahmood K, et al. A study of aerosol properties over Lahore (Pakistan) by using AERONET data. *Asia J Atmos Sci*. 2014;50:153-162.
45. Khan M, Tariq S, Haq ZU. Variations in the aerosol index and its relationship with meteorological parameters over Pakistan using remote sensing. *Environ Sci Pollut Res*. 2023;30:47913-47934.
46. Khokhar M, Yasmin N, Chishtie F, Shahid I. Temporal variability and characterization of aerosols across the Pakistan region during the winter fog periods. *Atmos*. 2016;7:67-18.
47. Kim KH, Ho DX, Park CG, et al. Volatile organic compounds in ambient air at four residential locations in Seoul, Korea. *Environ Eng Sci*. 2012;29:875-889.
48. Moreau M, Orange N, Feuilleley MG. Non-thermal plasma technologies: new tools for bio-decontamination. *Biotechnol Adv*. 2008;26:610-617.
49. Giardina A, Schiorlin M, Marotta E, Paradisi C. Atmospheric pressure non-thermal plasma for air purification: ions and ionic reactions induced by dc+ Corona discharges in air contaminated with acetone and methanol. *Plasma Chem Plasma Process*. 2020;40:1091-1107.
50. Belan M, Messanelli F. Compared ionic wind measurements on multi-tip corona and DBD plasma actuators. *J Electrostat*. 2015;76:278-287.
51. Maria SF, Russell LM, Turpin BJ, Porcja RJ. Ftir measurements of functional groups and organic mass in aerosol samples over the Caribbean. *Atmos Environ*. 2002;36:5185-5196.
52. Allen DT, Palen EJ, Haimov MI, Hering SV, Young JR. Fourier transform infrared spectroscopy of aerosol collected in a low pressure impactor (LPI/FTIR): method development and field calibration. *Aerosol Sci Technol*. 1994;21:325-342.
53. Martinez M, Baudelet M. Calibration strategies for elemental analysis of biological samples by LA-ICP-MS and LIBS – a review. *Anal Bioanal Chem*. 2020;412:27-36.
54. Wu P, Li J, Lu X, Tang Y, Cai Z. Release of tens of thousands of microfibers from discarded face masks under simulated environmental conditions. *Sci Total Environ*. 2022;806:150458-150466.
55. Bolaina-Lorenzo E, Puente-Urbina BA, Espinosa-Neira R, et al. A simple method to improve antibacterial properties in commercial face masks via incorporation of ZnO and CuO nanoparticles through chitosan matrix. *Mater Chem Phys*. 2022;287:126299-126304. doi:10.1016/j.matchemphys.2022.126299
56. Borkow G, Zhou SS, Page T, Gabbay J. A novel anti-influenza copper oxide containing respiratory face mask. *PLoS One*. 2010;5:11295-11303.
57. Marina-Montes C, Motto-Ros V, Pérez-Arribas LV, et al. Aerosol analysis by micro laser-induced breakdown spectroscopy: a new protocol for particulate matter characterization in filters. *Anal Chim Acta*. 2021;1181:338947-338956.
58. Singh VK, Sharma J, Pathak AK, Ghany CT, Gondal MA. Laser-induced breakdown spectroscopy (LIBS): a novel technology for identifying microbes causing infectious diseases. *Biophys Rev*. 2018;10:1221-1239.
59. Kaiser J, Novotný K, Martin MZ, et al. Trace elemental analysis by laser-induced breakdown spectroscopy—biological applications. *Surf Sci Rep*. 2012;67:233-243.
60. Després VR, Huffman JA, Burrows SM, et al. Primary biological aerosol particles in the atmosphere: a review. *Tellus B Chem Phys Meteorol*. 2012;64:15598-15657. doi:10.3402/tellusb.v64i0.15598
61. Shaltout AA, Boman J, Hassan SK, et al. Elemental composition of PM<sub>2.5</sub> aerosol in a residential-industrial area of a Mediterranean megacity. *Arch Environ Contam Toxicol*. 2020;78:68-78.
62. Whittaker A, Bérubé K, Jones T, Maynard R, Richards R. Killer smog of London, 50 years on: particle properties and oxidative capacity. *Sci Total Environ*. 2004;334-335:435-445.
63. Angyal A, Ferenczi Z, Manousakas M, et al. Source identification of fine and coarse aerosol during smog episodes in Debrecen, Hungary. *Air Qual Atmos Health*. 2021;14:1017-1032.
64. Kim KH, Jahan SA, Kabir E. A review on human health perspective of air pollution with respect to allergies and asthma. *Environ Int*. 2013;59:41-52.
65. Zhang B. The effect of aerosols to climate change and society. *J Geosci Environ Prot*. 2020;08:55-78.
66. Duarte RMBO, Duarte AC. Urban atmospheric aerosols: sources, analysis, and effects. *Atmos*. 2020;11:1221-1225.
67. Lasheras RJ, Paules D, Escudero M, et al. Quantitative analysis of major components of mineral particulate matter by calibration free laser-induced breakdown spectroscopy. *Spectrochim Acta Part B*. 2020;171:105918-105926.